Chapter 3

A moving boundary problem with space-fractional diffusion logistic population model and density-dependent dispersal rate

3.1 Introduction

A diffusion logistic population model including a moving boundary is one of the interesting moving boundary problems (Stefan problem) which deals with the study of spreading and vanishing of the species. In our ecological system, the case of spreading or vanishing of the species is a remarkable topic and several studies have been performed by many researchers to understand this natural phenomenon. Some of them are deliberated in [126, 127, 128]. In ecology, most of the mathematical models are based on presumption and usually, only a few empirical data are available to verify the models. In most of the cases, it is difficult and costly to collect useful field data by covering the vast areas. Due to these facts, the mathematical formulations of ecological problems are complicated. But, the mathematical formulation of a diffusion logistic population problem attracts many researchers and some notable achievement has been received to understand spreading and vanishing of the species through the model analogous to the classical moving boundary problem

[129, 130, 131, 132, 133]. The basic assumptions of these models are a thin tailed period of inactivity and thin tailed space for spreading/vanishing of the species.

Besides the classical problems, some processes occurring in nature that cannot be modelled with the aid of Fick's and Fourier's laws. Therefore, many models including fractional derivatives have been received in recent years for the different physical phenomenon like sediment transport problem [134], melting and freezing problem [135], the problem of drug release from polymer matrix [136], etc. The assumption of the formulation of these models is that the flux for some moment at a certain point depends on the distribution of the physical quantities at that point as well as the other points and their history. Gao et al. [136] discussed a problem with a moving boundary including space-fractional derivative in drug release devices and discussed a numerical solution of the problem by finite difference method. Some remarkable research associated with logistic model including fraction derivatives are also available in the literature [137, 138]. In this study, these facts inspire us to consider the space-fractional diffusion logistic population model. Recently, moving boundary problems with variable diffusivity have attracted many researchers [46, 111]. Kumar et al. [88] and Singh et al. [112] also discussed the models of moving boundary problems with variable thermal conductivity and heat capacity.

Motivated by the previous observations, the diffusive logistic population model with space derivative of fractional order is considered here to understand the spreading as well as the vanishing of invasive species. Moreover, it is assumed that the dispersal rate is of variable type, which depends on population density, and the expression of the dispersal rate is considered with the aid of Ims and Andreassen [139]. In this study, a numerical solution to the proposed model is presented with the help of the finite difference scheme with its stability and consistency criteria. In moving boundary problem, the presence of moving front and nonlinear nature makes it

difficult to establish its exact solution in many complex cases. Therefore, many approaches have been developed to find numerical solutions of such mathematical models and some of them are given in [99, 118, 123, 140]. In 2015, Lee et al. [141] discussed a numerical approach to a moving boundary problem which is a velocity-based moving mesh method. But, the numerical approaches also need a special caution to handle moving boundary problems. For some cases, very small mesh size and/or time step size are required to get a desired accuracy of the solutions [67]. Recently, Piqueras et al. [125] presented a numerical solution to a moving boundary problem associated with diffusion logistic population model. Liu et al. [142] discussed some numerical solutions of a class of reaction–diffusion equations including Stefan conditions. Zheng et al. [143] also presented a numerical solution to a time fractional reaction-diffusion model including a moving boundary. The numerical solution of fractional differential equation by finite difference scheme can also be seen in [144].

3.2 Mathematical Model

Motivated by [136, 125], the diffusive logistic population model with space derivative of fractional order and density-dependent dispersal rate is considered to understand the spreading as well as the vanishing of invasive species. The formulation of the problem is given below:

$$\frac{\partial U}{\partial \tau} - \digamma(U)\, {}_0^C D_z^\alpha U(z,\tau) = U(a-bU), \quad \tau > 0, \quad 0 < z < H(\tau), \quad 1 < \alpha \leqslant 2, \tag{3.1}$$

$$\frac{\partial U}{\partial z}(0,\tau) = 0, \tag{3.2}$$

$$U(H(\tau),\tau) = 0, \tag{3.3}$$

$$\frac{dH}{d\tau} = -\mu_0^C D_z^{\alpha-1} U(H(\tau),\tau), \tag{3.4}$$

$$H(0) = H_0, \quad U(z,0) = U_0(z) > 0, \quad 0 \leqslant z \leqslant H_0, \tag{3.5}$$

where U is the population density, τ is time, F is density dependent dispersal rate, $H(\tau)$ is moving boundary, μ is a non-negative parameter, a and b are positive constants. Here, the density-dependent dispersal rate [139] is considered as

$$F(U) = \frac{exp(c+dU)}{1+exp(c+dU)}, \tag{3.6}$$

where c and d are constants.

Here, $U_0(z)$ is taken as an initial function which satisfies the following condition:

$$U_0(z) \in C^2([0,H_0]), \quad \frac{\partial U_0}{\partial z}(0) = U_0(H_0) = 0, \quad 0 \leqslant z < H_0. \tag{3.7}$$

3.3 Numerical solution of the problem

First, the moving domain $[0, H(\tau)]$ is converted into the fixed domain $[0\ ,1]$ by using the following Landau-type transformation [99] and **Property 3** of Caputo derivative:

$$W(x,t) = U(z,\tau), \quad x = \frac{z}{H(\tau)}, \quad t = \tau, \tag{3.8}$$

$$\frac{\partial U}{\partial \tau} = \frac{\partial W}{\partial t} - \frac{x}{H(t)}\frac{dH}{dt}\frac{\partial W}{\partial x}, \tag{3.9}$$

$$ {}_0^C D_z^{\alpha} U(z,\tau) = \frac{1}{H^{\alpha}(t)} {}_0^C D_x^{\alpha} W(x,t), \tag{3.10} $$

$$ {}_0^C D_z^{\alpha-1} U(z,\tau) = \frac{1}{H^{\alpha-1}(t)} {}_0^C D_x^{\alpha-1} W(x,t). \tag{3.11} $$

Under the transformation (3.8) and by using (3.9)-(3.11), the Eqs. (3.1)-(3.5) reduce to the following system:

$$ \frac{\partial W}{\partial t} = \frac{x}{H(t)} \frac{dH}{dt} \frac{\partial W}{\partial x} + \frac{F(W)}{H^{\alpha}(t)} {}_0^C D_x^{\alpha} W(x,t) + W(a - bW), \quad 0 < x < 1, \quad 1 < \alpha \leqslant 2, \tag{3.12} $$

$$ \frac{\partial W}{\partial x}(0,t) = 0, \tag{3.13} $$

$$ W(1,t) = 0, \tag{3.14} $$

$$ \frac{dH}{dt} = -\frac{\mu}{H^{\alpha-1}(t)} {}_0^C D_x^{\alpha-1} W(1,t). \quad t > 0, \tag{3.15} $$

The initial conditions (3.5), variable dispersal rate (3.6) and Eq. (3.7) are transformed as

$$ H(0) = H_0, \quad W(x,0) = W_0(x) = U_0(xH_0), \quad 0 \leqslant x \leqslant 1, \tag{3.16} $$

$$ F(W) = \frac{exp(c + dW)}{1 + exp(c + dW)}, \tag{3.17} $$

and

$$ W_0(x) \in C^2([0,1]), \quad \frac{\partial W_0}{\partial x}(0) = W_0(1) = 0, \quad 0 \leqslant x < 1, \tag{3.18} $$

respectively.

Now, the step size of time discretization is considered as $k = \Delta t$ and space discretization $h = \Delta x = \frac{1}{N}$, where N is positive integer. The mesh points are taken as

(x_i, t^n), where $x_i = ih$, $0 \leqslant i \leqslant N$ and $t^n = nk$, $n \geqslant 0$. The approximate value of $W(x,t)$ at mesh point (x_i, t^n) is denoted as W_i^n, the approximate value of $H(t)$ at t^n is taken as H^n and also $F(W_i^n) = F_i^n$.

Let us approximate the time derivative and space derivative as

$$\frac{\partial W(x_i,t^n)}{\partial t} \approx \frac{W_i^{n+1} - W_i^n}{k}, \tag{3.19}$$

$$\frac{dH(t^n)}{dt} \approx \frac{H^{n+1} - H^n}{k}, \tag{3.20}$$

$$\frac{\partial W(x_i,t^n)}{\partial x} \approx \frac{W_{i+1}^n - W_{i-1}^n}{2h}. \tag{3.21}$$

The first order approximation for the fractional order derivative [144] is considered as

$$\begin{aligned} {}_0^C D_x^\alpha W(x_i,t^n) &= \frac{1}{\Gamma(2-\alpha)} \int_0^{x_i} \frac{\partial^2 W(x',t^n)}{\partial x'^2} \frac{dx'}{(x_i - x')^{\alpha-1}} = \frac{1}{\Gamma(2-\alpha)} \\ \int_0^{x_i} \frac{\partial^2 W(x_i - x',t^n)}{\partial x'^2} \frac{dx'}{x'^{\alpha-1}} &= \frac{1}{\Gamma(2-\alpha)} \sum_{j=0}^{i-1} \int_{x_j}^{x_{j+1}} \frac{\partial^2 W(x_i - x',t^n)}{\partial x'^2} \frac{dx'}{x'^{\alpha-1}} \\ \approx \frac{1}{\Gamma(2-\alpha)} \sum_{j=0}^{i-1} \frac{A_{ij}^n}{h^2} \int_{x_j}^{x_{j+1}} \frac{dx'}{x'^{\alpha-1}} &= \frac{(h)^{-\alpha}}{\Gamma(3-\alpha)} \sum_{j=0}^{i-1} e_j A_{ij}^n. \end{aligned} \tag{3.22}$$

$$\begin{aligned} {}_0^C D_x^{\alpha-1} W(x_i,t^n) &= \frac{1}{\Gamma(2-\alpha)} \int_0^{x_i} \frac{\partial W(x',t^n)}{\partial x'} \frac{dx'}{(x_i - x')^{\alpha-1}} = \frac{1}{\Gamma(2-\alpha)} \\ \int_0^{x_i} \frac{\partial W(x_i - x',t^n)}{\partial x'} \frac{dx'}{x'^{\alpha-1}} &= \frac{1}{\Gamma(2-\alpha)} \sum_{j=0}^{i-1} \int_{x_j}^{x_{j+1}} \frac{\partial W(x_i - x',t^n)}{\partial x'} \frac{dx'}{x'^{\alpha-1}} \\ \approx \frac{1}{\Gamma(2-\alpha)} \sum_{j=0}^{i-1} \frac{B_{ij}^n}{h} \int_{x_j}^{x_{j+1}} \frac{dx'}{x'^{\alpha-1}} &= \frac{(h)^{-\alpha+1}}{\Gamma(3-\alpha)} \sum_{j=0}^{i-1} e_j B_{ij}^n. \end{aligned} \tag{3.23}$$

where $e_j = [(j+1)^{2-\alpha} - j^{2-\alpha}]$, $A_{ij}^n = W(x_i - x_{j+1}, t^n) - 2W(x_i - x_j, t^n) + W(x_i -$

$x_{j-1}, t^n)$, $B_{ij}^n = W(x_i - x_j, t^n) - W(x_i - x_{j-1}, t^n)$, $1 < \alpha \leqslant 2$.

From Eqs.(3.19)-(3.22), the Eq.(3.12) is approximated as

$$\frac{W_i^{n+1} - W_i^n}{k} - \frac{x_i}{H^n}\Big(\frac{H^{n+1} - H^n}{k}\Big)\Big(\frac{W_{i+1}^n - W_{i-1}^n}{2h}\Big) - \frac{\digamma_i^n h^{-\alpha}}{(H^n)^\alpha \Gamma(3-\alpha)}$$
$$\sum_{j=0}^{i-1} e_j((W_{i-j+1}^n - 2W_{i-j}^n + W_{i-j-1}^n)) = W_i^n(a - bW_j^n),$$
$$n \geqslant 0, \quad 0 \leqslant i \leqslant N-1, \tag{3.24}$$

which can be rearranged as

$$W_i^{n+1} = \Big[\frac{k\digamma_i^n h^{-\alpha}}{(H^n)^\alpha \Gamma(3-\alpha)} + \frac{x_i}{H^n}\Big(\frac{H^{n+1} - H^n}{2h}\Big)\Big]W_{i-1}^n + \Big[1 + k(a - bW_i^n)$$
$$- \frac{2k\digamma_i^n h^{-\alpha}}{(H^n)^\alpha \Gamma(3-\alpha)}\Big]W_i^n + \Big[\frac{k\digamma_i^n h^{-\alpha}}{(H^n)^\alpha \Gamma(3-\alpha)} - \frac{x_i}{H^n}\Big(\frac{H^{n+1} - H^n}{2h}\Big)\Big]W_{i+1}^n$$
$$+ \frac{\digamma_i^n h^{-\alpha}}{(H^n)^\alpha \Gamma(3-\alpha)} \sum_{j=1}^{i-1} e_i(W_{i-j+1}^n - 2W_{i-j}^n + W_{i-j-1}^n),$$
$$n \geqslant 0, \quad 0 \leqslant i \leqslant N-1, \tag{3.25}$$

Eqs. (3.13) and (3.14), respectively become

$$\frac{W_1^n - W_0^n}{h} = 0, \tag{3.26}$$

and

$$W_N^n = 0. \tag{3.27}$$

Using first order forward difference approximation for time derivative and Eq.(3.23) for space discretization, the Stefan condition (3.15) becomes

$$\frac{H^{n+1}-H^n}{k} = \frac{-\mu}{(H^n)^{\alpha-1}}\frac{(h)^{-\alpha+1}}{\Gamma(3-\alpha)}\sum_{j=0}^{N-1} e_i(W^n_{N-i}-W^n_{N-i-1})), \quad n \geqslant 0, \tag{3.28}$$

The Eq.(5.37) can be rewritten as

$$H^{n+1} = H^n + \frac{\mu k}{(H^n)^{\alpha-1}}\frac{(h)^{-\alpha+1}}{\Gamma(3-\alpha)}\Big(W^n_{N-1} - \sum_{j=1}^{N-1} e_i(W^n_{N-i}-W^n_{N-i-1}))\Big), \quad n \geqslant 0. \tag{3.29}$$

Now, using Eq.(3.29) in the Eq.(3.25), we have

$$W_i^{n+1} = a_i^n W_{i-1}^n + b_i^n W_i^n + c_i^n W_{i+1}^n + \frac{k\mu x_i h^{-\alpha}}{2(H^n)^{\alpha}\Gamma(3-\alpha)}\sum_{j=1}^{N-1} e_j(W^n_{N-j}-W^n_{N-j-1})$$
$$(W^n_{i-1}-W^n_{i+1}) + \frac{k\digamma_i^n h^{-\alpha}}{(H^n)^{\alpha}\Gamma(3-\alpha)}\sum_{j=1}^{i-1} e_j(W^n_{i-j+1}-2W^n_{i-j}+W^n_{i-j-1}), \tag{3.30}$$

where

$$a_i^n = \Big[\frac{k\digamma_i^n h^{-\alpha}}{(H^n)^{\alpha}\Gamma(3-\alpha)} - \frac{k\mu x_i h^{-\alpha}}{2(H^n)^{\alpha}\Gamma(3-\alpha)}W^n_{N-1}\Big], \tag{3.31}$$

$$b_i^n = \Big[1 + k(a-bW_i^n) - \frac{2k\digamma_i^n h^{-\alpha}}{(H^n)^{\alpha}\Gamma(3-\alpha)}\Big], \tag{3.32}$$

$$c_i^n = \Big[\frac{k\digamma_i^n h^{-\alpha}}{(H^n)^{\alpha}\Gamma(3-\alpha)} + \frac{k\mu x_i h^{-\alpha}}{2(H^n)^{\alpha}\Gamma(3-\alpha)}W^n_{N-1}\Big], \quad n \geqslant 0, \quad 1 \leqslant i \leqslant N-1. \tag{3.33}$$

3.4 Consistency

The consistency of a numerical technique depends upon the problem [118, 125], therefore, here the consistency of the numerical scheme for the considered problem is

discussed. A finite difference method is consistent with a partial differential equation when truncation error goes to zero as step-size approaches to zero.

The vector form of Eqs.(3.12)-(3.16) is denoted as

$$\mathcal{X}(\mathcal{Y}(x,t),\mathcal{H}(t)) = (\mathcal{X}_1(\mathcal{Y}(x,t),\mathcal{H}(t)),\mathcal{X}_2(\mathcal{Y}(x,t),\mathcal{H}(t)),\mathcal{X}_3(\mathcal{Y}(x,t),\mathcal{H}(t))), \quad (3.34)$$

where

$$\begin{aligned}\mathcal{X}_1(\mathcal{Y},\mathcal{H}) &= \frac{\partial \mathcal{Y}}{\partial t} - \frac{x}{\mathcal{H}(t)}\frac{d\mathcal{H}}{dt}\frac{\partial \mathcal{Y}}{\partial x} - \frac{\digamma(\mathcal{Y})}{\mathcal{H}^{\alpha}(t)}{}_0^C D_x^{\alpha}\mathcal{Y}(x,t) \\ &\quad - \mathcal{Y}(a-b\mathcal{Y}) = 0, \quad t>0, \quad 0<x<1, 1<\alpha\leqslant 2 \qquad (3.35)\\ \mathcal{X}_2(\mathcal{Y},\mathcal{H}) &= \frac{\partial W}{\partial x}(0,t) = 0, \quad t>0, \qquad (3.36)\\ \mathcal{X}_3(\mathcal{Y},\mathcal{H}) &= \frac{d\mathcal{H}}{dt} + \frac{\mu}{\mathcal{H}^{\alpha-1}(t)}{}_0^C D_x^{\alpha-1}\mathcal{Y}(1,t), \quad t>0. \qquad (3.37)\end{aligned}$$

The vector form of the difference scheme Eqs. (3.24), (3.26) and (3.28) are denoted and defined as

$$X(W,H) = (X_1(W,H), X_2(W,H), X_3(W,H)), \quad (3.38)$$

where X_1, X_2 & X_3 are defined at mesh point (x_i, t^n) as

$$\begin{aligned}X_1(W_i^n, H^n) &= \frac{W_i^{n+1}-W_i^n}{k} - \frac{x_i}{H^n}\Big(\frac{H^{n+1}-H^n}{k}\Big)\Big(\frac{W_{i+1}^n - W_{i-1}^n}{2h}\Big) \\ &\quad + \frac{\digamma_i^n h^{-\alpha}}{(H^n)^{\alpha}\Gamma(3-\alpha)}\sum_{j=0}^{i} e_i(W_{i-j+1}^n - 2W_{i-j}^n + W_{i-j-1}^n) \\ &\quad - W_i^n(a-bW_j^n), \quad n\geqslant 0, \quad 0\leqslant i\leqslant N-1, \qquad (3.39)\end{aligned}$$

$$X_2(W_i^n, H^n) = \frac{W_1^n - W_0^n}{h} = 0, \tag{3.40}$$

$$X_3(W_i^n, H^n) = \frac{H^{n+1} - H^n}{k} + \frac{\mu}{(H^n)^{\alpha-1}} \frac{(h)^{-\alpha+1}}{\Gamma(3-\alpha)} \sum_{j=0}^{N-1} e_j (W_{N-j}^n - W_{N-j-1}^n)),$$

$$n \geqslant 0. \tag{3.41}$$

According to [118] and [125], the local truncation error $E_i^n(\mathcal{Y}, \mathcal{H})$ is defined as

$$E_i^n(\mathcal{Y}, \mathcal{H}) = (E(1)_i^n, E(2)_i^n, E(3)_i^n), \tag{3.42}$$

where

$$E(1)_i^n = X_1(\mathcal{Y}_i^n, \mathcal{H}^n) - \mathcal{X}_1(\mathcal{Y}_i^n, \mathcal{H}^n), \tag{3.43}$$

$$E(2)_i^n = X_2(\mathcal{Y}_i^n, \mathcal{H}^n) - \mathcal{X}_2(\mathcal{Y}_i^n, \mathcal{H}^n), \tag{3.44}$$

$$E(3)_i^n = X_3(\mathcal{Y}_i^n, \mathcal{H}^n) - \mathcal{X}_3(\mathcal{Y}_i^n, \mathcal{H}^n), \tag{3.45}$$

In Eqs. (3.43)-(3.45), $\mathcal{Y}_i^n = \mathcal{Y}(x_i, t^n)$, and $\mathcal{H}^n = \mathcal{H}(t^n)$ are taken as the exact values at the mesh point (x_i, t^n) of the solutions of the Eqs.(3.12)-(3.16). It is clear that when $h \to 0$ and $k \to 0$, the local truncation error $E_i^n(\mathcal{Y}, \mathcal{H})$ goes to 0 and hence, our numerical solution $X(\mathcal{Y}, \mathcal{H})$ is consistent with $\mathcal{X}(\mathcal{Y}, \mathcal{H})$. Next, it is assumed that $\mathcal{Y}(x, t)$ is four times continuously partial differentiable with respect to x and two times w.r.t. t. Moreover, it is considered that $\mathcal{H}(t)$ is continuously differentiable two times w.r.t. t.

Now, Taylor's expansion of $X_1(\mathcal{Y}_i^n, \mathcal{H}^n)$ about (x_i, t^n) is used in Eq.(3.43) which gives:

$$E(1)_i^n = T_i^n(1)k - \frac{x_i}{\mathcal{H}^n}\mathcal{H}'(t^n)T_i^n(2)h^2 - \frac{x_i}{\mathcal{H}^n}\frac{\partial \mathcal{Y}}{\partial x}(x_i, t^n)T_i^n(3)k - \frac{x_i}{\mathcal{H}^n}T_i^n(2)T^n(3)kh^2 - \frac{F_i^n h^{3-\alpha}}{(\mathcal{H}^n)^\alpha}T_i^n(4), \tag{3.46}$$

where

$$T_i^n(1) = \frac{1}{2}\frac{\partial^2 \mathcal{Y}}{\partial t^2}(x_i, \delta), \quad t^n < \delta < t^{n+1}, \tag{3.47}$$

$$T_i^n(2) = \frac{1}{6}\frac{\partial^3 \mathcal{Y}}{\partial x^3}(\Psi_1, t^n), \quad x_{i-1} < \Psi_1 < x_{i+1}, \tag{3.48}$$

$$T^n(3) = \frac{1}{2}\frac{d^2 \mathcal{H}}{dt^2}(\Lambda), \quad t^n < \Lambda < t^{n+1}, \tag{3.49}$$

$$|T_i^n(4)| \leqslant \frac{2\Psi_2^{2-\alpha}}{\Gamma(3-\alpha)}, \quad x_{i-1} < \Psi_2 < x_{i+1}. \tag{3.50}$$

Clearly, the local truncation error becomes

$$E(1)_i^n(\mathcal{Y}, \mathcal{H}) = \mathcal{O}(k) + \mathcal{O}(h^{3-\alpha}). \tag{3.51}$$

In the similar manner, the following can be written as

$$E(2)_i^n(\mathcal{Y}, \mathcal{H}) = \mathcal{O}(h), \tag{3.52}$$

by substituting Eqs.(3.36) and (3.40) in the Eq.(3.44), and the following equation can be obtained by using Eqs.(3.37), (3.41) in the Eq.(3.45):

$$E(3)_i^n(\mathcal{Y}, \mathcal{H}) = \mathcal{O}(k) + \mathcal{O}(h^{3-\alpha}). \tag{3.53}$$

3.5 Stability

3.5.1 Positiveness

When we work on the population density model, then we have to ensure that the numerical solution of our model is non-negative. This section has two parts. In the first part, the non-negative nature of the model is discussed, while in the second part the stability of our solution has been discussed.

With the help of induction method on index n, the non-negative nature of our solution W_i^n (given in (3.30)) and monotonicity of H_n (3.29) are shown. If $n = 0$ then from Eq. (3.18), we have $W_i^0 > 0$, $0 \leqslant i \leqslant N-1$. For small h, the difference approximation $\frac{(W_{N-2}^n - 4W_{N-1}^n + 3W_N^n)}{2h} = \frac{(W_{N-2}^n - 4W_{N-1}^n)}{2h} < 0$ by taking the left derivative of $W_0'(1^-)$ at $z = 1$ in Eq. (3.18).

Since, $H^0 > 0$ therefore from (3.29), we get:

$$H^1 > H^0 > 0.$$

Now, assume that $W_i^p > 0$ and $H^p > H^{p-1} > \cdots > H^0 > 0$ for $1 \leqslant p \leqslant n$. In order to prove the positivity and monotonicity of the solution, it is required to show that $W_i^{n+1} > 0$ and $H^{n+1} > H^n$.

As given in [125], the Taylor's expansion about $x_N = 1$ give rise to

$$W_{N-2}^n = 2W_{N-1}^n + \mathcal{O}(h^2), \quad n \geqslant 0. \tag{3.54}$$

From Eq. (3.29) and by using $W_{N-1}^n = \mathcal{O}(h)$, we get

$$\begin{aligned} H^{n+1} &= H^n + \frac{k\mu h^{-\alpha}}{(H^n)^{\alpha-1}\Gamma(3-\alpha)}\Big(W_{N-1}^n - \sum_{j=1}^{N-1} e_j(W_{N-j}^n - W_{N-j-1}^n\Big), \\ &= H^n + \mathcal{O}(k), \quad n \geqslant 0. \end{aligned} \tag{3.55}$$

which is similar to the results concluded from [125].

Now, let us come back to the positiveness of the solution. Taking $i = N-1$ in Eqs. (3.30) - (3.33) and Eq. (3.54), we get

$$W_{N-1}^{n+1} = (1 + k(a - bW_{N-1}^n) - \frac{kx_i\mu h^{-\alpha}}{(H^n)^{\alpha}\Gamma(3-\alpha)}W_{N-1}^n)W_{N-1}^n + \mathcal{O}(h^{3-\alpha}). \tag{3.56}$$

According to the assumption $H^n > H^0$ and $x_{N-1} < 1$, the (3.56) reduces to

$$W_{N-1}^{n+1} > (1 + k(a - bW_{N-1}^n) - \frac{k\mu h^{-\alpha}}{(H^0)^{\alpha}\Gamma(3-\alpha)}W_{N-1}^n)W_{N-1}^n = \psi_{N-1}^n W_{N-1}^n. \tag{3.57}$$

for small h. To show the positivity of W_{N-1}^n, we must show that $\psi_{N-1}^n > 0$ by bounding W_{N-1}^n. For small h, the Eq. (3.56) produces $W_{N-1}^{p+1} < W_{N-1}^p(1+ka)$ for $0 \leqslant p \leqslant n-1$ and recursively we get

$$W_{N-1}^n < W_{N-1}^0(1+ka)^{p+1} < e^{aT}W_{N-1}^0, \quad 0 \leqslant p \leqslant n \leqslant M-1, \quad kM = T, \tag{3.58}$$

for $T > 0$.

By using Eq. (3.58) and expression of ψ_{N-1}^n, we have $W_{M-1}^n > 0$ when

$$k < \frac{h^{\alpha}}{\frac{\mu P}{(H^0)^{\alpha}\Gamma(3-\alpha)} + h^{\alpha}(bP - a)}, \tag{3.59}$$

where

$$P = e^{aT} W_{N-1}^{0}. \tag{3.60}$$

The positivity of W_{N-1}^{n} has been proved under the condition (3.59). Now, we have to prove that $W_i^n > 0$ for $0 \leqslant i \leqslant N-2$ and this is possible when the assumption of induction and all positive coefficients of Eq. (3.30) are considered. By considering Eq. (3.31) and taking into account that $0 \leqslant x_i < 1$, every coefficients of $a_i^n > 0$ if $W_{N-1}^n < \frac{2F_i^n}{\mu}$. In view of Eq. (3.60), we can say that $a_i^n > 0$ under the following condition:

$$W_{N-1}^{0} < \frac{2F_i^n e^{-aT}}{\mu}. \tag{3.61}$$

Again from Eq. (3.33), the coefficients $c_i^n > 0$ for small h. As given in [125], let us define $K(n)$ as $K(n) = max\{w_i^n : 0 \leqslant i \leqslant n\}$. Now by using the assumption of induction, we have $H^n > H^0 > 0$. Hence, $b_i^n > 0$ for $i > 0$ if

$$k < \frac{h^\alpha}{\frac{2F_i^n}{(H^0)^\alpha \Gamma(3-\alpha)} + h^\alpha (bK(n) - a)}. \tag{3.62}$$

From the positivity of the coefficients a_i^n, b_i^n, c_i^n and Eq. (3.30), we have

$$\begin{aligned} W_i^{n+1} &\leqslant (1 + k(a - bW_i^n))K(n) \leqslant (1 + ka)K(n) \leqslant (1 + ka)^2 K(n-1) \\ &\leqslant \cdots \leqslant (1 + ka)^{n+1} K(0) < e^{aT} K(0), \quad 0 \leqslant n \leqslant M-1, \quad kM = T, \end{aligned} \tag{3.63}$$

where $K(0) = max\{W(x_i, 0), 0 \leqslant i \leqslant N\}$, $0 \leqslant x_i \leqslant 1$. From (3.29) and (3.54), we have $H^{n+1} > H^n$ which proves the monotonicity of the moving boundary H^n.

As given in [125], the following result is considered:

Theorem 3.1. *Let us define* k_0 *as:*

$$k_0 = min\Big\{k_1 = \frac{h^\alpha}{\frac{\mu P}{(H^0)^\alpha \Gamma(3-\alpha)} + h^\alpha(bP-a)}, \quad k_2 = \frac{h^\alpha}{\frac{2F_i^n}{(H^0)^\alpha \Gamma(3-\alpha)} + h^\alpha(be^{aT}K(0)-a)}\Big\}. \tag{3.64}$$

If $k < k_0$ *and* h *is sufficiently small then the solution* $\{W_i^n,\, H^n\}$ *given in Eqs.* (3.26), (3.27), (3.29) *and* (3.30) *shows that* H^n *is a positive monotonically increasing and*

$$0 \leqslant W_i^n \leqslant e^{aT}K(0), \quad 0 \leqslant i \leqslant N, \quad 0 \leqslant n \leqslant M, \quad kM = T. \tag{3.65}$$

3.5.2 Stability

As given in [125], the infinity norm ($\|.\|_\infty$) is assumed to define stability criteria which is given below.

Definition 3.2. In the domain $[0,1]\times[0,T]$, the numerical technique (3.28)-(3.30) is $\|.\|_\infty$-stable for each partition with h and k if

$$\|W^n\|_\infty \leqslant L\|W^0\|_\infty, \qquad 0 \leqslant n \leqslant M, \tag{3.66}$$

where $\|W^n\|_\infty$=max$(|W_0^n|, |W_1^n|, \ldots, |W_N^n|)$ and L is independent from h, k and n.

By considering Eq. (3.65), Theorem 3.1 and taking into account that $K(n) = \|W^n\|_\infty$, we have

$$\|W^n\|_\infty \leqslant L\|W^0\|_\infty,$$

where $L = e^{aT}$. Thus, we have the following result:

Theorem 3.3. *In the domain* $[0,1] \times [0,T]$*, the numerical technique* (3.28)-(3.30) *is conditionally* $\|.\|_\infty$*-stable for sufficiently small* h *and* $k < k_0$*, where* k_0 *is given in Eq.* (3.64)

3.6 Convergence

The convergence of the proposed numerical technique is discussed here.

Theorem 3.4. *If* $k < k_0$*, then the numerical technique* (3.24) *is convergent for the space-fractional diffusion logistic population model* (3.12)-(3.17)*, and the order of convergence is* $\mathcal{O}(k + h^{3-\alpha})$*.*

Proof Let $W_i^n = \mathcal{Y}_i^n - E_i^n$ and $\mathcal{H}^n = \mathcal{H}(t^n)$,

where W_i^n is approximate solution, $\mathcal{Y}_i^n = \mathcal{Y}(x_i, t^n)$ is the exact solution and E_i^n is the error.

From (3.24), we have

$$\frac{(\mathcal{Y}_i^{n+1} - \mathcal{Y}_i^n) - (E_i^{n+1} - E_i^n)}{k} - \frac{x_i}{\mathcal{H}^n}\Big(\frac{\mathcal{H}^{n+1} - \mathcal{H}^n}{k}\Big)\Big(\frac{(\mathcal{Y}_{i+1}^n - \mathcal{Y}_{i-1}^n) - (E_{i+1}^n - E_{i-1}^n)}{2h}\Big)$$
$$+ \frac{F_i^n h^{-\alpha}}{(\mathcal{H}^n)^\alpha \Gamma(3-\alpha)} \sum_{j=0}^{i-1} e_j \Big((\mathcal{Y}_{i-j+1}^n - 2\mathcal{Y}_{i-j}^n + \mathcal{Y}_{i-j-1}^n) - (E_{i-j+1}^n - 2E_{i-j}^n + E_{i-j-1}^n)\Big)$$
$$= (\mathcal{Y}_i^n - E_i^n)(a - b(\mathcal{Y}_i^n - E_i^n)), \quad n \geqslant 0, \quad 0 \leqslant i \leqslant N-1. \tag{3.67}$$

Now, the Taylor's series expansion in Eq. (3.67) is used which gives

$$\Big(\frac{\partial \mathcal{Y}(x_i,t^n)}{\partial t}+\mathcal{O}(k)-\frac{(E_i^{n+1}-E_i^n)}{k}\Big)-\frac{x_i}{\mathcal{H}^n}\Big(\frac{d\mathcal{H}(t^n)}{dt}+\mathcal{O}(k)\Big)\Big(\frac{\partial \mathcal{Y}(x_i,t^n)}{\partial x}+\mathcal{O}(h^2)-\frac{(E_{i+1}^n-E_{i-1}^n)}{2h}\Big)+\frac{F_i^n}{(\mathcal{H}^n)^\alpha}\Big({}_0^C D_x^\alpha \mathcal{Y}(x_i,t^n)+\mathcal{O}(h^{3-\alpha})\Big)-\frac{\digamma_i^n h^{-\alpha}}{(\mathcal{H}^n)^\alpha\Gamma(3-\alpha)}$$
$$\sum_{j=0}^{i-1} e_j(E_{i-j+1}^n-2E_{i-j}^n+E_{i-j-1}^n)=(\mathcal{Y}_i^n-E_i^n)(a-b(\mathcal{Y}_i^n-E_i^n)),$$
$$n\geqslant 0,\quad 0\leqslant i\leqslant N-1. \tag{3.68}$$

Thus, Eq. (3.12) and Eq. (3.68) produce

$$\frac{(E_i^{n+1}-E_i^n)}{k}-\frac{x_i}{\mathcal{H}^n}\frac{d\mathcal{H}(t^n)}{dt}\frac{(E_{i+1}^n-E_{i-1}^n)}{2h}+\frac{\digamma_i^n h^{-\alpha}}{(\mathcal{H}^n)^\alpha\Gamma(3-\alpha)}\sum_{j=0}^{i-1} e_j(E_{i-j+1}^n-$$
$$2E_{i-j}^n+E_{i-j-1}^n)\leqslant E_i^n(a-bE_i^n)+\mathcal{O}(k)+\mathcal{O}(h^{3-\alpha}),\quad n\geqslant 0,\quad 0\leqslant i\leqslant N-1, \tag{3.69}$$

or

$$E_i^{n+1}\leqslant (1+k(a-bE_i^n))E_i^n-\frac{kx_i}{\mathcal{H}^n}\frac{d\mathcal{H}(t^n)}{dt}\frac{(E_{i+1}^n-E_{i-1}^n)}{2h}+\frac{k\digamma_i^n h^{-\alpha}}{(\mathcal{H}^n)^\alpha\Gamma(3-\alpha)}$$
$$\sum_{j=0}^{i-1} e_j(E_{i-j+1}^n-2E_{i-j}^n+E_{i-j-1}^n)+k(\mathcal{O}(k+h^{3-\alpha})),\quad n\geqslant 0,\quad 0\leqslant i\leqslant N-1. \tag{3.70}$$

Let $\mathcal{E}^n=max\{E_i^n: 0\leqslant i\leqslant N\}$, then

$$\mathcal{E}^{n+1}\leqslant (1+k(a-b\mathcal{E}^n))\mathcal{E}^n+k(\mathcal{O}(k+h^{3-\alpha}))\leqslant (1+ka)\mathcal{E}^n+k(\mathcal{O}(k+h^{3-\alpha})). \tag{3.71}$$

Hence,

$$\begin{aligned}||\mathcal{E}^{n+1}||_\infty &\leqslant (1+ka)||\mathcal{E}^n||_\infty + k(\mathcal{O}(k+h^{3-\alpha})) \leqslant (1+ka)^2||\mathcal{E}^{n-1}||_\infty + (1+ka)k(\mathcal{O}(k+h^{3-\alpha})+ \\ &\leqslant \cdots \leqslant (1+ka)^{n+1}||\mathcal{E}^0||_\infty + (1+ka)^n k(\mathcal{O}(k+h^{3-\alpha})) \\ &\leqslant Lk(\mathcal{O}(k+h^{3-\alpha})). \end{aligned} \tag{3.72}$$

Consequently, $|E_i^{n+1}| \to 0$ as $h \to 0$ and $k \to 0$ which proves that W converges to $\mathcal{Y}$ when $k < k_0$. Moreover, it is seen from Eq. (3.72) that the global error of the method is of order $\mathcal{O}(k + h^{3-\alpha})$.

3.7 Results and Discussions

Theoretical results at $\alpha = 2$ has been established for spreading as well as vanishing cases in [128] and these results are also verified numerically [125]. In [128], it is observed that spreading occurs when $H_0 \geqslant L$, where $L = \frac{\pi}{2}\sqrt{\frac{F}{a}}$. On the other hand if $H_0 < L$, the spreading occurs when $\mu > \mu^*$, where μ^* is unknown threshold which depends on W_0 (see Theorem 3.9 of [128]). As the time approaches infinity, the population density in spreading case approaches to habitat carrying capacity a/b (see Lemma 3.2 of [128]). In the case of $H_0 < L$ and $\mu \leqslant \mu^*$ the population density starts vanishing when $H(t) \leqslant L$ for $t > 0$.

In this study, the above conditions are assumed and solve the problem (3.1)-(3.5) for different values of α. In our knowledge, the exact solution of the problem (3.1)-(3.5) is not available in the literature, therefore a numerical solution of the problem is discussed and obtained results are presented through figures. For all computations, the stability of the technique is achieve by taking grid size $h = 0.05$ ($N = 20$ *or* $\Delta x = \frac{1}{20}$) and the time step $k = 0.0001$.

In Figs. 3.1 - 3.12, the dependence of population density and moving boundary on various time τ are shown for different density-dependent dispersal rate $F(U)$ and α. Figs 3.1 - 3.6 represent the variation of population of species with time for different values of α while dispersal rate is density-dependent. Figs. 3.1 - 3.3 depict the case of spreading of population density for three different values of α (α=1.4, 1.6, 1.8) at the parameters $a = 3$, $b = 2$, $c = 1$, $d = 1$, μ=1 and H_0=2 by taking initial function $U_0 = \cos(\pi z/4)$. From these figures, it is observed that the population density reaches to habitat carrying capacity when we increase the time. Moreover, it is seen that the population density covers small space domain to reach the habitat carrying capacity when α increases for a fixed time ($t > 2$). Figs. 3.4 - 3.6 represent the the case of vanishing of the species for three different values of α (α=1.4, 1.6, 1.8) for the parameters $a = 0.02$, $b = 0.02$, $c = 1$, $d = 1$, μ=0.2, H_0=2 by considering initial function $U_0 = \cos(\pi z/4)$. Figs 3.4 - 3.6 show that the process of vanishing of population density becomes slow when we increase the value of α as time proceeds.

Figs. 3.7 - 3.11 represent the effect of density-dependent dispersal rate over the constant dispersal rate on $U(z, \tau)$ and $H(\tau)$. In order to show the effect of density-dependent dispersal rate, here constant dispersal rate=1 is considered because for the positive values of c and d, $F(U) \approx 1$. Fig. 3.7 represent the comparison of population density for density-dependent and constant dispersal rate for spreading case at the parameters α=2, $a = 1$, $b = 1$, $c = 1$, $d = 1$, μ=2 and H_0=2 with the initial function $U_0 = \cos(\pi z/4)$. This figure shows that the population density curve is more near to the habitat carrying capacity in the case of density-dependent dispersal rate than the constant dispersal rate. Fig. 3.8 is plotted for the comparison of population density for density-dependent and constant dispersal rate for vanishing case at the parameters α=2, $a = 1$, $b = 1$, $c = 1$, $d = 1$, μ=0.1 and H_0=2 with the initial function $U_0 = \cos(\pi z/4)$. In this figure, it is observed that the population

density vanishes faster for the case of constant dispersal rate than density-dependent dispersal rate. Figs. 3.9 and 3.10 show the trajectory of moving boundary for different value of α (α=1.4, 1.7, 2.0) by considering density-dependent dispersal rate and constant dispersal rate, respectively at parameters $a = 1$, $b = 1$, $c = 1$, $d = 1$, μ=0.5, H_0=2 and $U_0 = \cos(\pi z/4)$. Figs. 3.9 and 3.10 demonstrate that the speed of moving boundary becomes slow when we increase the value of α. But, the movement of moving boundary is faster for the case of density-dependent dispersal rate than the case of constant dispersal rate. Fig. 3.11 represents the comparison of tracking of the moving boundary between density-dependent dispersal rate and constant dispersal rate for different values of μ (μ=1.0, 1.5, 2.0) and it is plotted for parameters α=2, $a = 1$, $b = 1$, $c = 1$, $d = 1$, H_0=1 and initial function $U_0 = \cos(\pi z/2)$. From this figure, it is observed that the moving boundary in the case of density-dependent dispersal rate moves faster than the case of constant dispersal rate.

Fig. 3.12 is plotted for the tracking of moving boundary by considering density-dependent dispersal rate at α=2 (standard case) for different values of μ to estimate μ^* (threshold). This figure is plotted for the parameters $a = 1$, $b = 1$, $c = 1$, $d = 1$, H_0=1 and initial function $U_0 = \cos(\pi z/2)$.

Fig. 3.13 is plotted to show the behaviour of $|W^{n+1} - W^n| = max|W_i^{n+1} - W_i^n|$, $1 \leqslant i \leqslant N - 1$ with n for three different values of α ($\alpha = 1.4, 1.6, 2.0$) at the parameters $a = 1$, $b = 1$, $c = 1$, $d = 1$, $H_0 = 1$, $\mu = 0.5$ and initial function $U_0 = \cos(\pi z/4)$. From this figure, it is clear that $|W^{n+1} - W^n|$ decreases as n increases for all values of α, $1 < \alpha \leqslant 2$.

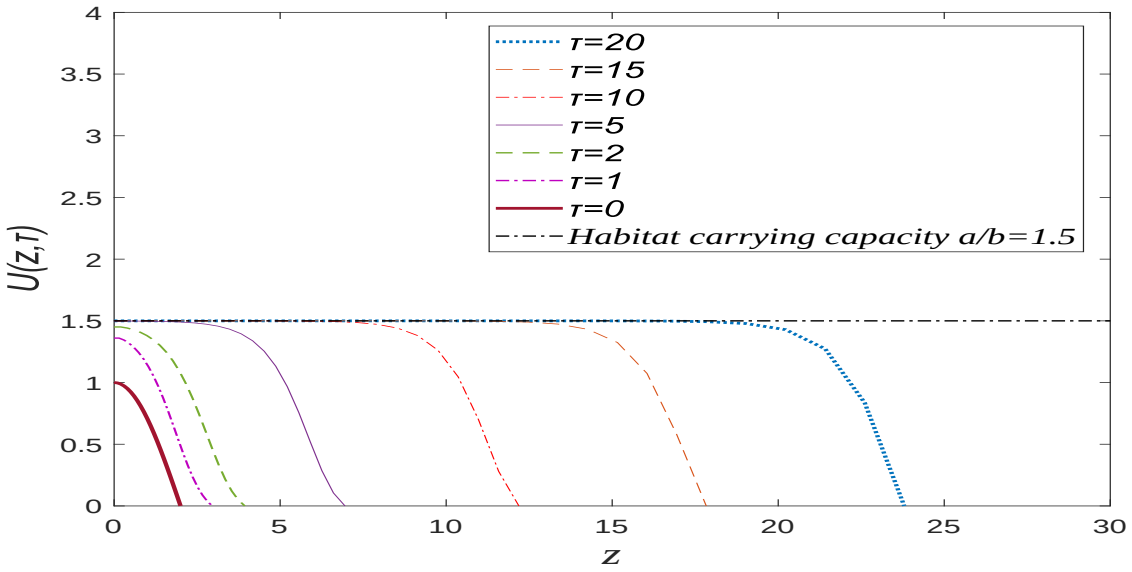

FIGURE 3.1: Spreading of population density for α=1.4.

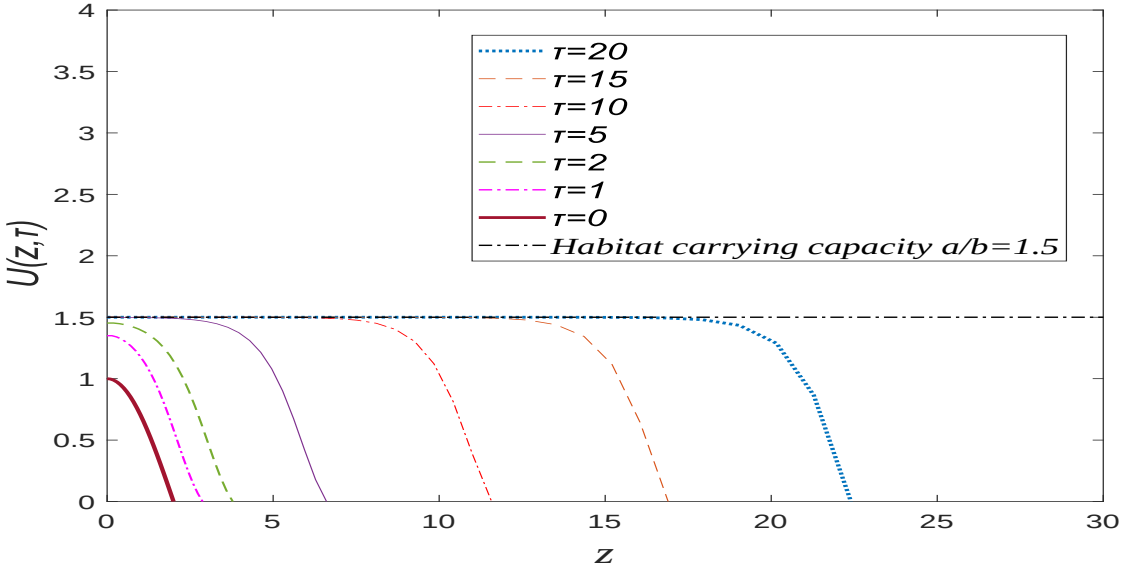

FIGURE 3.2: Spreading of population density for α=1.6.

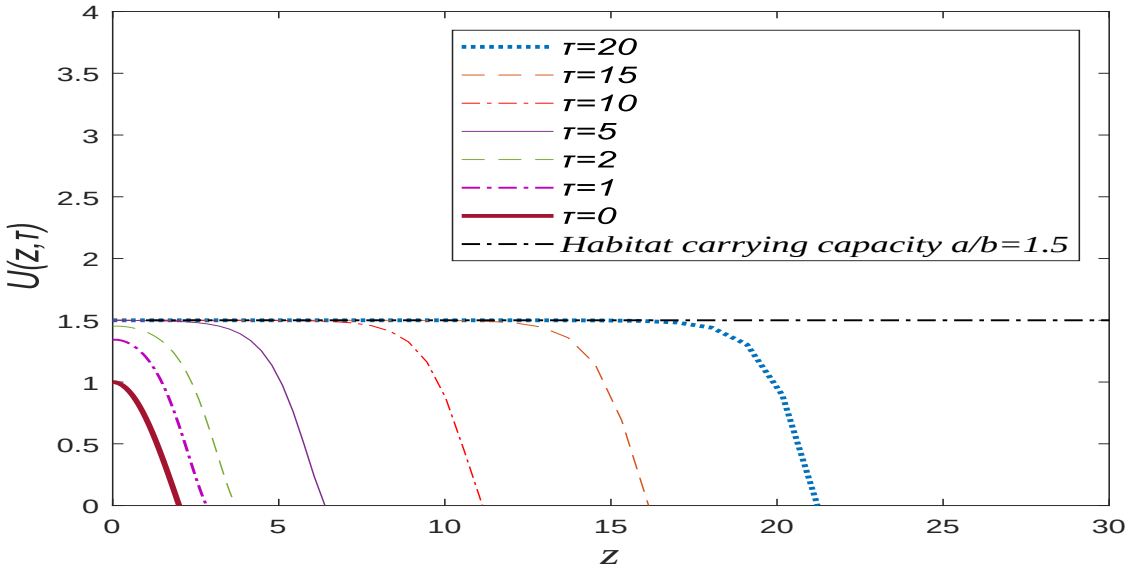

FIGURE 3.3: Spreading of population density for α=1.8.

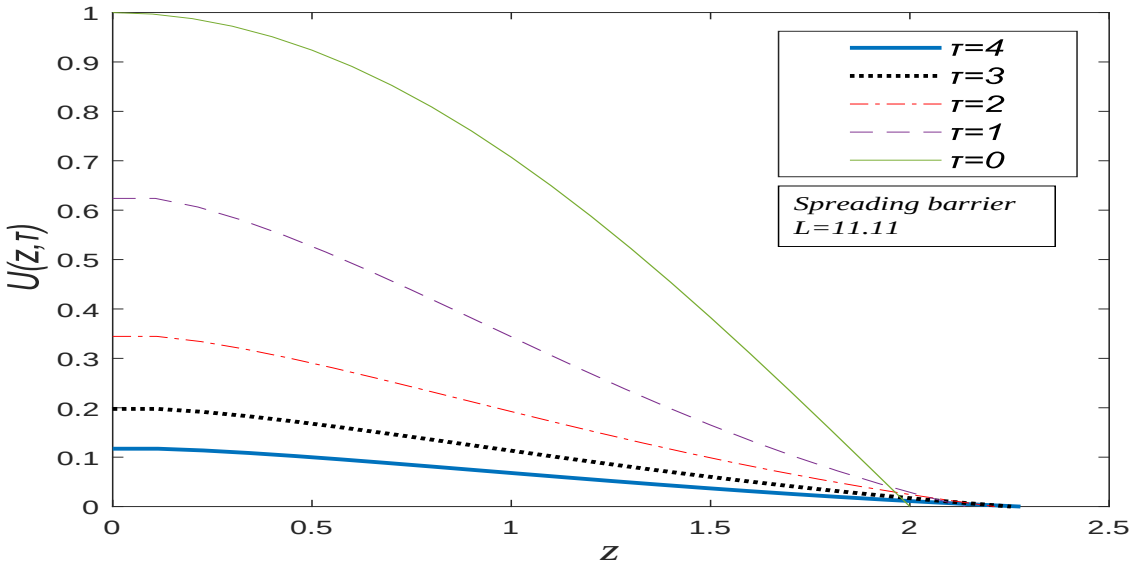

FIGURE 3.4: Vanishing of population density for α=1.4.

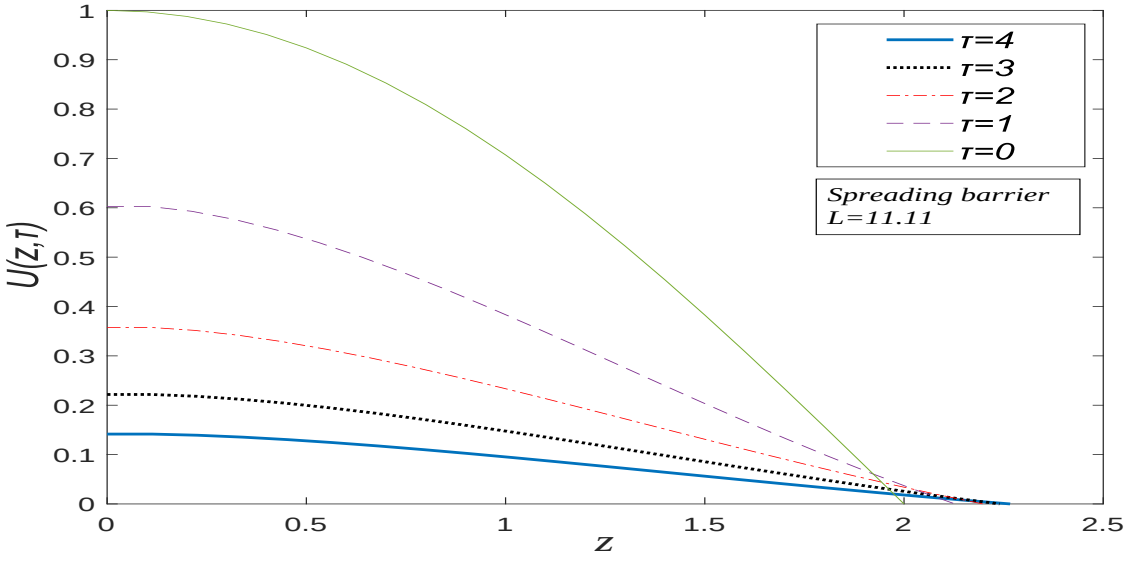

FIGURE 3.5: Vanishing of population density for α=1.6.

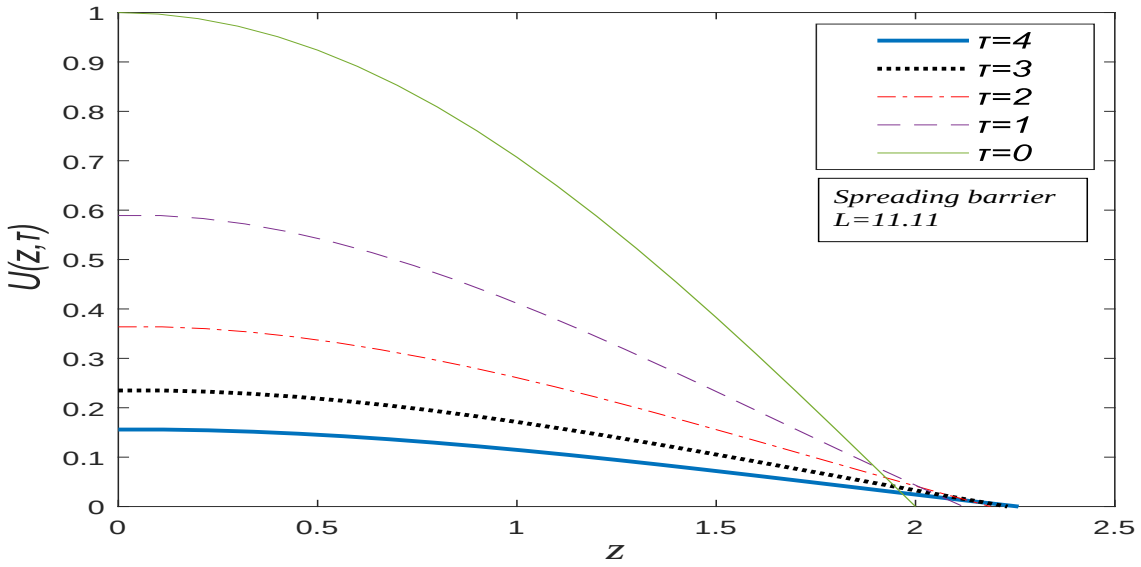

FIGURE 3.6: Vanishing of population density for α=1.8.

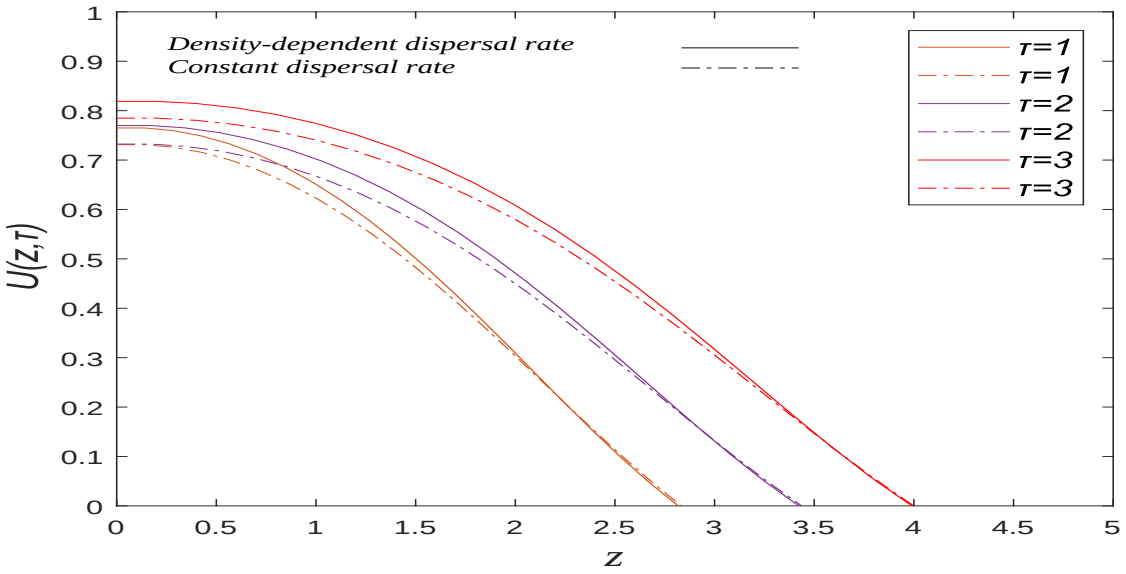

FIGURE 3.7: Comparison of spreading population density for density-dependent and constant dispersal rate at α=2.

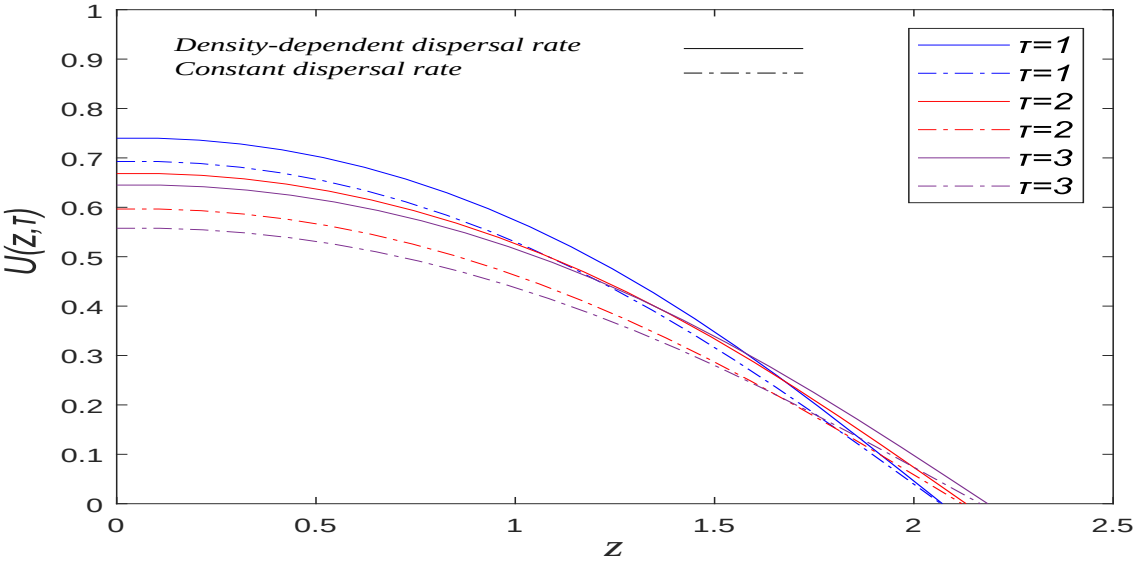

FIGURE 3.8: Comparison of vanishing population density for density-dependent and constant dispersal rate at α=2.

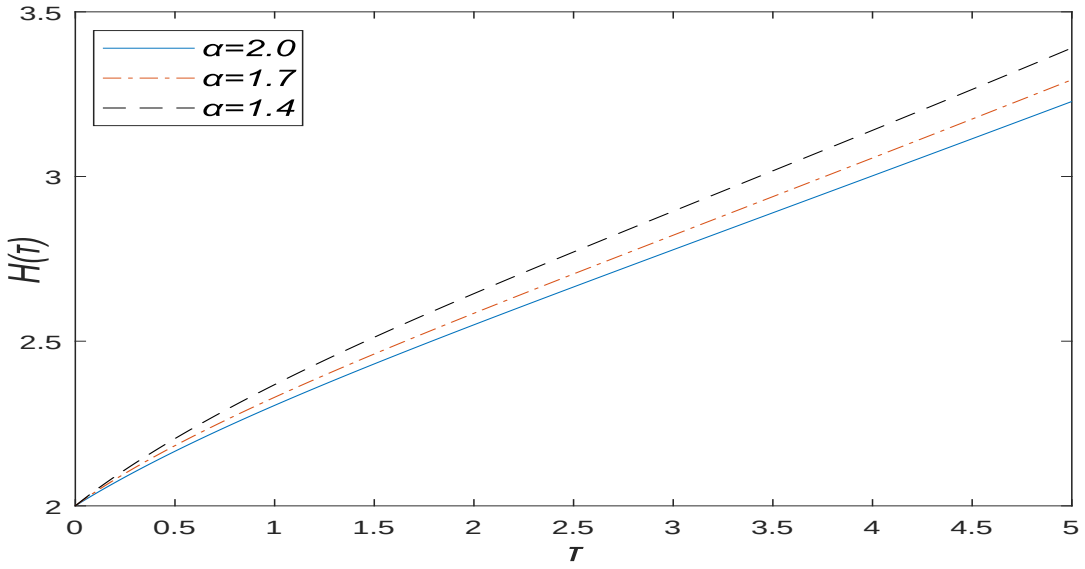

FIGURE 3.9: Trend of moving boundary for different values of α in the case of density-dependent dispersal rate.

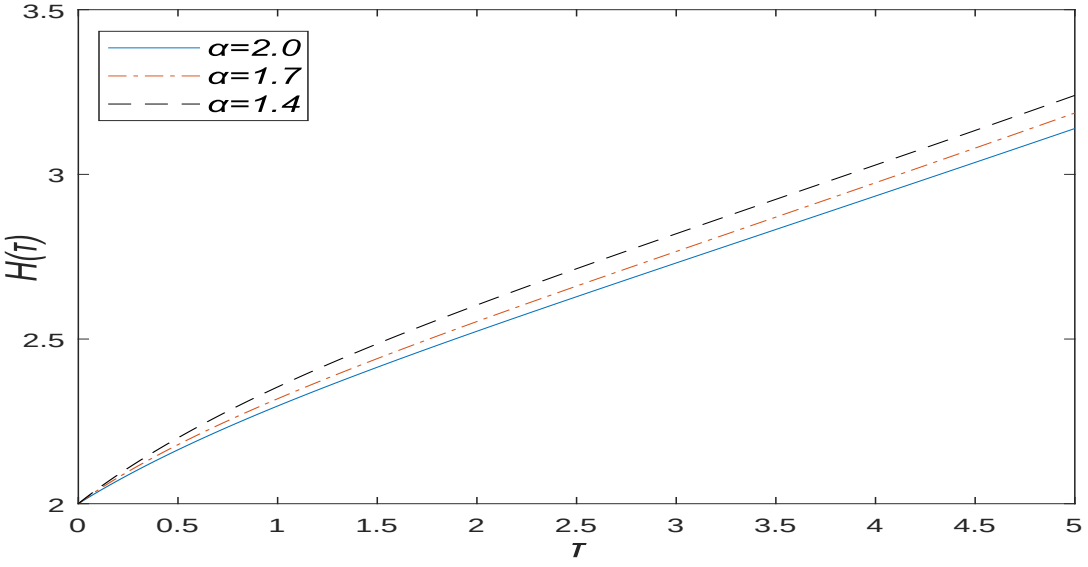

FIGURE 3.10: Trend of moving boundary for different values of α in the case of constant dispersal rate.

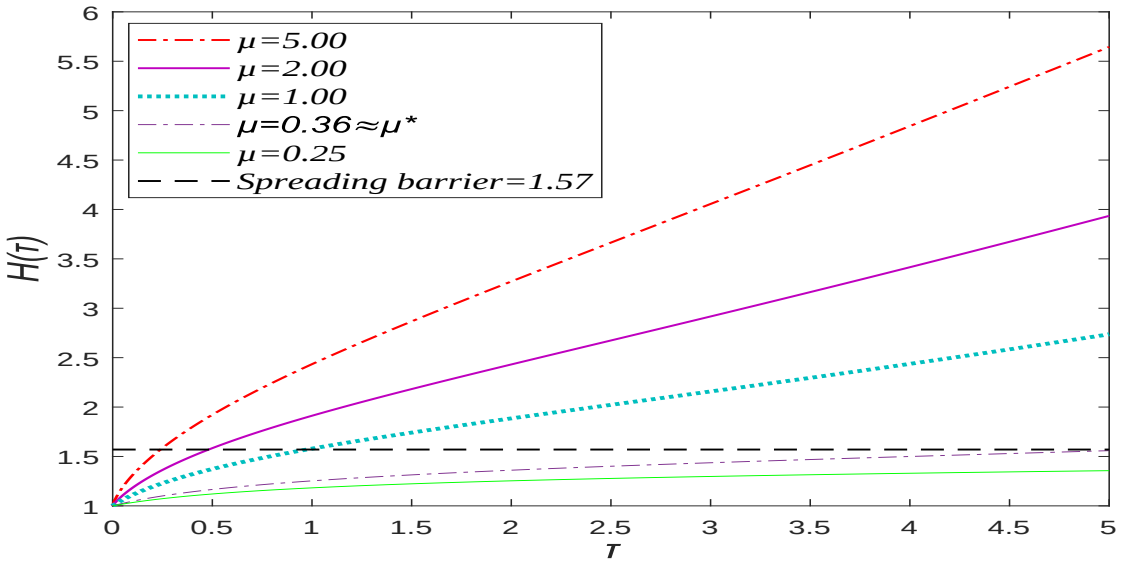

FIGURE 3.11: Comparison of moving boundary for different values of μ.

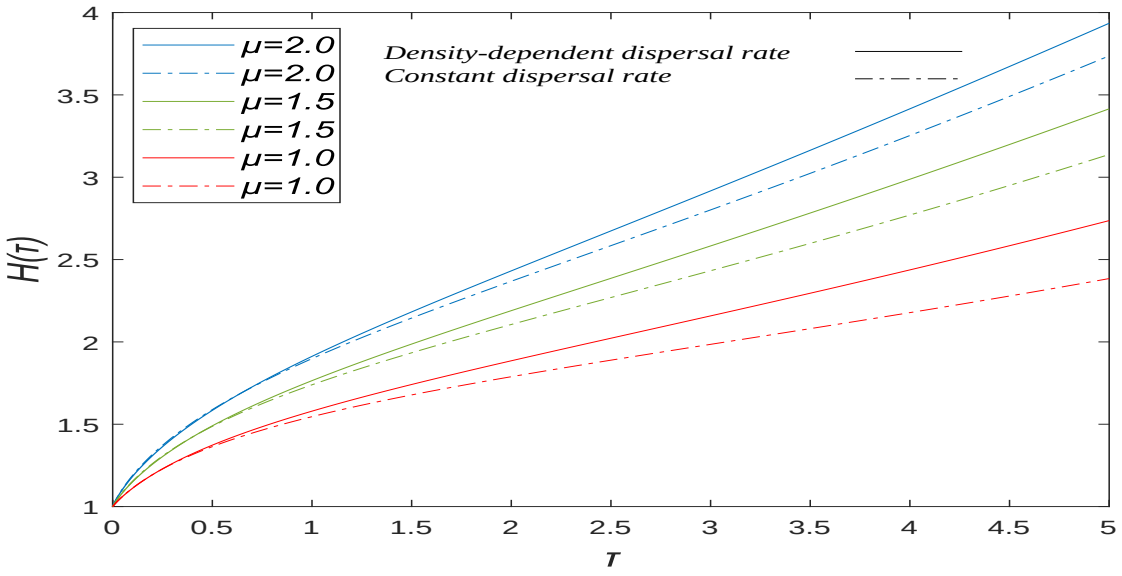

FIGURE 3.12: Trend of moving boundary for different values of μ.

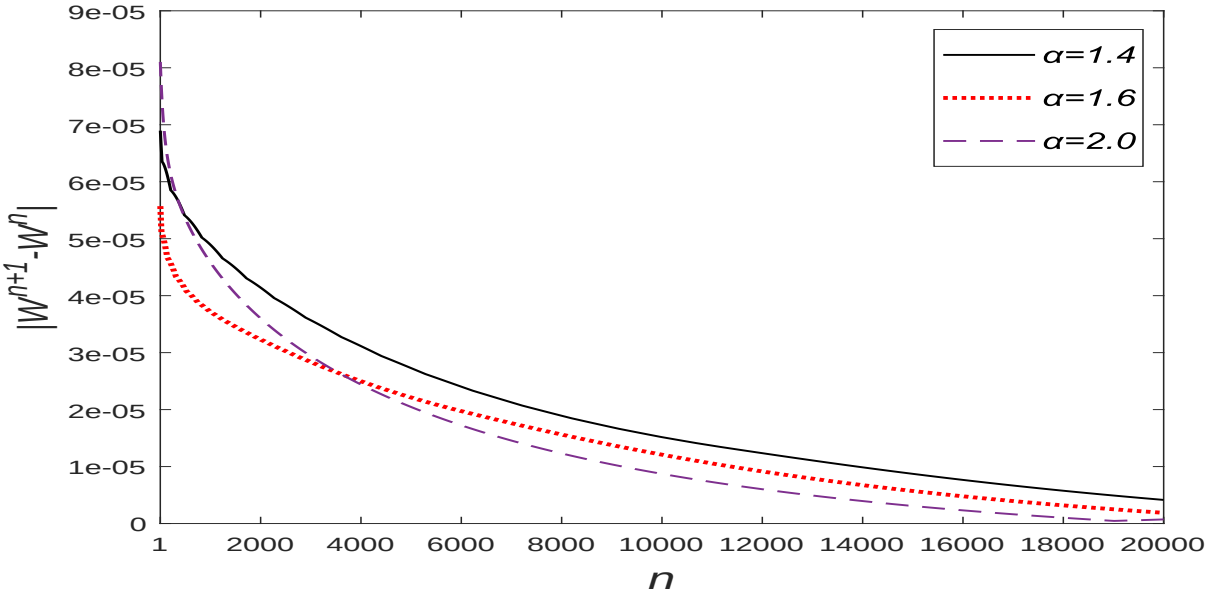

FIGURE 3.13: Trend of $|W^{n+1} - W^n|$ as n increases for different values of α.

3.8 Conclusion

In this chapter, a finite difference scheme is applied to present a numerical solution of a population logistic diffusion model with fractional order space derivative and density-dependent dispersal rate. From this study, it is observed that the numerical approach is simple and efficient scheme for the solution of wide class of a nonlinear diffusion model with moving boundary. It is found that the population density is affected by the density-dependent dispersal rate ($F(U)$) and α. For spreading case, it is observed that the population density reaches to the habitat carrying capacity faster in case of density-dependent dispersal rate than the constant dispersal rate and it is also seen that the population density covers small space domain to reach the habitat carrying capacity when α increases. For the vanishing case, it is found that the population density vanishes faster for the case of constant dispersal rate in comparison to density-dependent dispersal rate and it is also observed that the

process of the vanishing of the population density become slow with the increment in the value of α. Density-dependent dispersal rate also affects the expanding front and the expanding front moves faster when we consider the density-dependent dispersal rate in our model. The parameter μ^* (threshold) is calculated in our case to confirm the occurrence of spreading and vanishing cases.

****